Biochimica et Biophysica Acta 1798 (2010) 376–388

Contents lists available at ScienceDirect

Biochimica et Biophysica Acta

journal homepage: www.elsevier.com/locate/bbamem

A calorimetric and spectroscopic comparison of the effects of ergosterol and cholesterol on the thermotropic phase behavior and organization of dipalmitoylphosphatidylcholine bilayer membranes☆

David A. Mannock, Ruthven N.A.H. Lewis, Ronald N. McElhaney *

Department of Biochemistry, University of Alberta, Edmonton, Alberta, Canada T6G 2H7

ARTICLE INFO

Article history:
Received 25 May 2009
Received in revised form 6 August 2009
Accepted 6 September 2009
Available online 15 September 2009

Keywords:
Ergosterol
Cholesterol
Dipalmitoylphosphatidylcholine
Thermotropic phase behavior
Sterol-lipid interactions
Lipid bilayer
Lipid membranes
Differential scanning calorimetry
Fourier transform infrared spectroscopy

ABSTRACT

We performed comparative DSC and FTIR spectroscopic measurements of the effects of cholesterol (Chol) and ergosterol (Erg) on the thermotropic phase behavior and organization of DPPC bilayers. Ergosterol is the major sterol in the biological membranes of yeasts, fungi and many protozoa. It differs from Chol in having two additional double bonds, one in the steroid nucleus at C7–8 and another in the alkyl chain at C22–23. Erg also has an additional methyl group in the alkyl chain at C24. Our DSC studies indicate that the incorporation of Erg is more effective than Chol is in reducing the enthalpy of the pretransition. At lower concentrations Erg is also more effective than Chol in reducing the enthalpies of both the sharp and broad components of main phase transition. However, at sterol concentrations from 30 to 50 mol%, Erg is generally less effective at reducing the enthalpy of the broad components and does not completely abolish the cooperative hydrocarbon chain-melting phase transition at 50 mol%, as does Chol. Nevertheless, in this higher ergosterol concentration range, there is no evidence of the formation of ergosterol crystallites. Our FTIR spectroscopic studies demonstrate that Erg incorporation produces a similar ordering of liquid-crystalline DPPC bilayers as does Chol, but an increased degree of hydrogen bonding of the fatty acyl carbonyl groups in the glycerol backbone region of the DPPC bilayer. These and other results indicate that Erg is less miscible in DPPC bilayers at higher concentrations than is Chol. Finally, we provide a tentative molecular explanation for the comparative experimental and computation results obtained for Erg and Chol in phospholipid bilayers, emphasizing the dynamic conformational differences between these two sterols.

1. Introduction

Cholesterol (Chol) is a major and essential lipid component of the plasma membranes of the cells of higher animals and is also found in lower concentrations in certain intracellular membranes in vesicular communication with the plasma membrane [1–3]. Although Chol has a number of different functions in animal cells, one of its primary roles is as a modulator of the physical properties and lateral organization of the plasma membrane lipid bilayer. In particular, the presence of Chol significantly increases the orientational order of the phospholipid hydrocarbon chains and decreases the cross-sectional area occupied by the phospholipid molecules, while only moderately restricting the rates of phospholipid lateral diffusion or hydrocarbon chain motion. As well, the presence of Chol increases both the thickness and mechanical strength and decreases the permeability of the phospholipid bilayer in the physiologically relevant L_α phase, producing a so-called L_o phase with a degree of organization intermediate between L_β and L_α phases [2,5–10].

Erg is the major sterol found in the plasma membranes of fungi and yeast [1]. As illustrated in Fig. 1, Erg differs from Chol in having an additional double bond in ring B of the steroid nucleus, as well as a double bond between C22–C23 and an extra methyl group at C24 of the alkyl side chain. The additional double bond and methyl group in the alkyl side chain of Erg will produce a more conformationally restricted rigid alkyl moiety and the additional conjugated double bond of the steroid nucleus may produce a more rigid and planar ring B and a flatter conformation of rings B and C. Moreover, the predominant conformers of Erg have an alkyl chain which protrudes

Abbreviations: PC, phosphatidylcholine; DPPC, dipalmitoylphosphatidylcholine; DMPC, dimyristoylphosphatidylcholine; POPC, 1-palmitoyl-2-oleoyl-phosphatidylcholine; DEPC, dielaidoylphosphatidylcholine; SpM, sphingomyelin; Chol, cholesterol; Erg, ergosterol; Lano, lanosterol; DSC, differential scanning calorimetry; FTIR, Fourier transform infrared; NMR, nuclear magnetic resonance; T_p, the pretransition temperature maximum; T_m, the main transition temperature maximum; ΔH, the transition enthalpy; $\Delta T_{½}$, the width of the phase transition at half height, inversely related to the cooperativity of the phase transition; $L_{\beta'}$ and L_β, lamellar gel phases with tilted and untilted hydrocarbon chains, respectively; $P_{\beta'}$, rippled gel phase with tilted hydrocarbon chains; L_α or L_d, lamellar liquid-crystalline or liquid-disordered phase; L_O, lamellar liquid-ordered phase; Erg-BC1 and Erg-BC2, first and second broad endotherm components of the ergosterol-DPPC DSC thermograms

☆ Supported by operating and major equipment grants from the Canadian Institutes of Health Research and by major equipment grants from the Alberta Heritage Foundation for Medical Research.

* Corresponding author. Tel.: +1 780 492 2413; fax: +1 780 492 0886.
E-mail address: rmcelhan@ualberta.ca (R.N. McElhaney).

0005-2736/$ – see front matter © 2009 Elsevier B.V. All rights reserved.
doi:10.1016/j.bbamem.2009.09.002

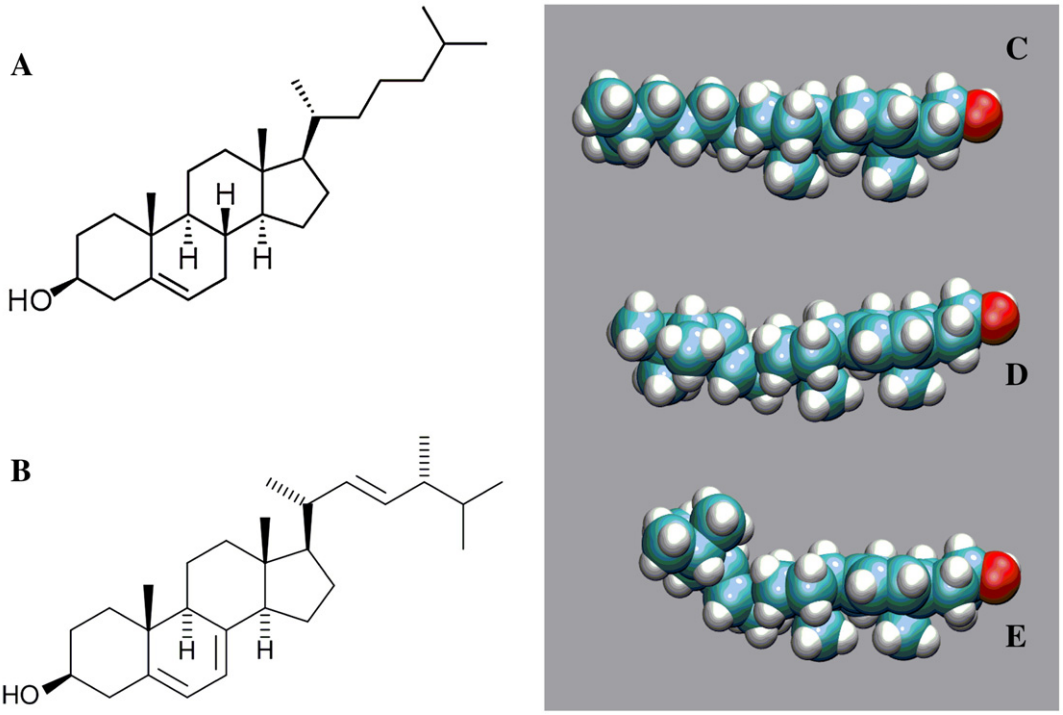

Fig. 1. Molecular models of cholesterol and ergosterol. The left panel shows line diagrams to highlight the differences between the structures of the cholesterol (A) and ergosterol (B) molecules. The right panel shows space-filling models illustrating the extended conformation of cholesterol (C), along with an extended conformation (D) and a bent (E) conformation of ergosterol.

at an angle to the plane of the steroid ring system in contrast to Chol, where the alkyl side chain is, on average, coplanar with the ring system [11]. Nonetheless, molecular dynamics simulations suggest that Erg occupies a considerably smaller effective molecular volume in DMPC [12] and DPPC [13] bilayers in the liquid-ordered state (but see [14]), probably due to both the lower off-axial mobility of the steroid nucleus and the alkyl side chain in Erg as compared to Chol, and to the greater condensing effect of Erg on the host phospholipid bilayer. In this regard, a quasi-elastic neutron scattering study indicates that in liquid-ordered DPPC/sterol (30 mol% sterol) bilayers, Erg has a lower lateral diffusion coefficient and a higher diffusion anisotropy than Chol, and an amplitude of out-of-plane motion more than a factor of 3 lower than Chol [15]. These results suggest that the bulkier and stiffer alkyl chain of Erg restricts its molecular motion in fluid phospholipid bilayers as compared to Chol. Finally, a ^{13}C NMR study reported that at 30 mol% sterol in DMPC/sterol vesicles, the molecular diffusion axis of Erg makes an angle of 14° to the inertial axis of the rigid four-ring system of this sterol, whereas in Chol the molecular diffusion and inertial steroid nucleus axes coincide [16], which supports the suggestion of a bent conformation of Erg [11].

Although Erg has not been studied experimentally nearly as extensively as Chol, nevertheless a number of studies have been carried out on Erg-phospholipid systems, many of which do not seem to be in agreement with one another. For example, Erg has been reported to be much less effective than Chol in condensing liquid-expanded unsaturated egg PC monolayers [4,17] or in reducing the permeability of liquid-crystalline egg PC liposomes to various permeants [18], and Erg has been reported to be much less soluble in fluid soybean PC vesicles than Chol [19]. Similarly, electron paramagnetic studies, utilizing doxyl fatty acid and cholestane spin label probes in egg PC vesicles, reported that Erg and Chol both comparably order the membrane up to concentration of 15–20 mol% sterol, but that Erg actually disorders the egg PC hydrocarbon chains at higher concentrations while Chol continues to increase hydrocarbon chain order up to 50 mol% [19,20]. Moreover, a fluorescence polarization study of sterol-containing fluid POPC membranes also found that whereas Erg and Chol comparably order the hydrocarbon chains up to 20 mol% sterol, the effect of Erg essentially plateaus at higher concentrations, whereas Chol continues to increase order up to a concentration of 50 mol% [21]. However, another steady-state fluorescence anisotropy study of fluid DPPC membranes reported that Erg is more effective than Chol in ordering this saturated phospholipid bilayer at all sterol levels studied up to 50 mol%, although this difference is most pronounced at lower sterol concentrations [22]. Still another fluorescence polarization study reported that Erg is less disordering in DPPC bilayers in the gel-state than is Chol [23]. Moreover, several NMR studies have reported that Erg is more effective than Chol in ordering the hydrocarbon chains of liquid-crystalline DMPC [24,25], POPC [25] or DPPC [26] bilayers at sterol levels of up to 25–30 mol%. However, at sterol concentrations of 40 mol%, Erg was reported to be less effective than Chol in increasing hydrocarbon chain order in DPPC bilayers [13,14]. Finally, in a multinuclear NMR study of POPC vesicles, Erg was reported to be less effective than Chol in ordering the hydrocarbon chain at sterol levels up to 25 mol%; moreover, at higher Erg concentrations, a second form of Erg was detected, suggesting Erg aggregation or phase separation [24]. Finally, a recent FITR spectroscopic study of fluid DPPC liposomes containing 28 mol% sterol reported that Erg is slightly more effective than Chol in ordering the hydrocarbon chains of this saturated phospholipid [27]. Overall, these various results suggest that Erg has a lower solubility limit in both saturated and especially mixed-chain saturated-unsaturated phospholipid bilayers than does Chol, and that Erg is more effective than Chol in ordering saturated but less effective in ordering unsaturated phospholipid membranes, below this miscibility limit.

A small number of comparative studies of the effects of Erg and Chol on other physical properties of phospholipid bilayers have also been carried out. For example, in DPPC/sterol (40 mol% sterol) membranes, micropipette aspiration and solid-state NMR studies indicate that Erg-containing bilayers are mechanically stiffer and less compressible than Chol-containing bilayers [28]. However, another micropipette aspiration study reported that Erg was less affective than

Chol in condensing DPPC bilayers at lower concentrations, but equally effective at higher concentrations [29]. In contrast, Erg was reported to produce a much smaller increase in lateral tension and surface viscosity of DEPC/sterol (40 mol% sterol) membranes than does Chol [30], and in POPC/sterol membranes, Erg produces a smaller increase in membrane order and bending rigidity than does Chol [29]. Moreover, in the latter study, vesicle fluctuation analysis indicates that the effects of Erg again tended to plateau about 20 mol% sterol, as found in earlier NMR and micropipette studies. However, another micropipette aspiration study reported that Chol and Erg import a similar condensation to DPPC bilayers [31]. Moreover, a molecular acoustic and calorimetric study of DPPC bilayers containing various concentrations of Chol and Erg reported essentially identical effects of these two sterols on the isothermal compressibility of the host membranes, although Erg was found to be more effective than Chol in promoting Lo phase formation [32]. As well, a small angle neutron scattering study of DMPC/sterol mixtures containing 20 and 47 mol% sterol demonstrated that Erg produces a lower bilayer compressibility relative to Chol, indicating a greater condensing effect [33], although increases in bilayer thickness are essentially identical with both sterols. Finally, Erg was reported to be more effective than Chol in inducing liquid-ordered domains in PC/sphingomyelin/sterol bilayers than is Chol [34–36]. It is possible that some of the experimental discrepancies in the literature arose from the use of rather impure Erg, especially in older studies.

High-sensitivity DSC is a nonperturbing thermodynamic technique which has proven of great value in studies of the effect of Chol and Chol analogs on the thermotropic phase behavior of phospholipid and sphingolipid bilayers [37–44]. However, there appear to have been only two DSC studies of Erg/phospholipid model membranes to date and neither of these have provided a detailed analysis of the DSC thermograms illustrated [27,32]. We have thus reinvestigated the effect of Erg and Chol on the thermotropic phase behavior of the well-studied DPPC bilayers using a high-sensitivity calorimeter and an experimental protocol which ensures that the broad, lower enthalpy phase transitions occurring at higher sterols levels are accurately monitored, using a very pure Erg preparation. Moreover, we have also investigated the effects of Erg and Chol incorporation on the organization of DPPC bilayers by FTIR spectroscopy. Overall, our results indicate that the effects of Erg on the thermotropic phase behavior and organization of DPPC vesicles are somewhat different from and more complex than those of Chol.

2. Materials and methods

The DPPC and Chol were both obtained from Avanti Polar Lipids Inc. (Alabaster, AL), whereas the Erg was supplied by Steraloids Inc. (Newport, RI). The purities of DPPC, Chol and Erg were >99%. All organic solvents were of at least analytical grade quality and were redistilled before use. Samples for hydration were prepared exactly as described previously [44]. The DPPC:sterol films were subsequently dispersed in an appropriate volume of deionized water by vigorous vortex mixing at temperatures near 55–60 °C. This procedure avoids any fractional crystallization of sterol during sample preparation.

The samples used for the DSC experiments were prepared by dispersing appropriate amounts of the dried lipid:sterol mixture in 1 ml of deionized water. The dispersion was then degassed and 324 μl aliquots were withdrawn for DSC analyses. To ensure better resolution of the broad low-enthalpy thermotropic transitions exhibited by sterol-rich mixtures, the amount of lipid used for DSC measurements was progressively increased with the sterol content of the mixture [40,45]. Typically, samples containing 1–3 mg phospholipid were used at sterol concentrations below 5 mol%, 5–8 mg phospholipid at sterol concentrations between 5 and 15 mol%, and 10–15 mg of phospholipid at all higher sterol concentrations. DSC heating and cooling thermograms were recorded with a high-sensitivity Nano II DSC (Calorimetry Sciences Corporation, Lindon, UT) operating at a scan rate of 10 °C/h. The data acquired were analyzed and plotted with the Origin software package (OriginLab Corporation, Northampton, MA). In cases where the DSC thermograms appeared to be a summation of overlapping components, the midpoint temperatures, areas and widths of the components were estimated with the aid of the Origin non-linear least squares curve- and peak-fitting procedures and a custom-coded function based on the assumption that the observed thermogram is a linear combination of components, each of which could be approximated by a reversible two-state transition at thermodynamic equilibrium. The equations used to develop the fitting function are described by Lewis et al. [45].

Samples used for FTIR spectroscopy were prepared by dispersing dried lipid:sterol mixtures containing 2–3 mg of phospholipid in 50 μl of distilled water at temperatures near 55–60 °C. The paste obtained was then sealed as a thin (25 μm) film between the CaF_2 windows of a heatable, demountable liquid cell equipped with a 25 μm Teflon spacer. Once mounted in the sample holder of the instrument, sample temperature could be controlled between −20 and 90 °C by means of an external computer-controlled water bath. FTIR spectra were acquired with a Digilab FTS-40 Fourier-transform spectrometer (Biorad, Digilab Division, Cambridge, MA) using data acquisition and data processing protocols described by previously [46].

3. Results

3.1. The overall pattern of thermotropic phase behavior observed in cholesterol/DPPC and ergosterol/DPPC multilamellar liposomes

Fig. 2 shows DSC heating scans of DPPC dispersions containing differing concentrations of both sterols. The overall pattern of thermotropic phase behavior seen on heating is similar to that reported previously for Chol/DPPC [37–43] and Erg/DPPC [27,32]. Pure DPPC heating scans show two sharp endothermic peaks centered at 34 °C and 41.2 °C, which correspond to the pretransition ($L_{\beta'}/P_{\beta'}$) and main ($P_{\beta'}/L_{\alpha}$) phase transition, respectively. Increasing the sterol concentration gradually broadens the pretransition and reduces its temperature and enthalpy in both cases. Similarly, in the case of the main phase transition, increasing the sterol concentration initially produces a multicomponent DSC endotherm, consisting of a sharp component that is progressively reduced in temperature, enthalpy and cooperativity, and a broad component that increases in both temperature and enthalpy, but decreases in cooperativity. Thus, with increasing sterol concentrations, the sharp component disappears as the broad component grows. However, there are subtle but significant differences in the pattern of thermal events observed in the Chol/DPPC (Fig. 2A) and Erg/DPPC (Fig. 2B) samples, which indicate that the behavior of the latter is more complex. We will first focus on the effect of both sterols on the pretransition and then on the major components of main phase transition of DPPC.

3.2. The effects of cholesterol and ergosterol on the pretransition of DPPC

In order to investigate the disappearance of the pretransition in greater detail, we prepared sterol/DPPC samples with a narrower range of Erg concentrations. The gradual elimination of the pretransition in the DSC heating scans of Erg/DPPC samples compared with corresponding thermograms of Chol/DPPC mixtures are shown in Fig. 3 and the derived thermodynamic measurements for both sterol/DPPC systems are presented in Fig. 4. The Chol/DPPC and Erg/DPPC samples show comparable decreases in the T_p (Fig. 4A, B) with increasing sterol concentration, with those of the Erg/DPPC mixtures being slightly greater than those of the Chol/DPPC samples at concentrations above 5 mol%. While the values of T_p decrease at similar rates, the values

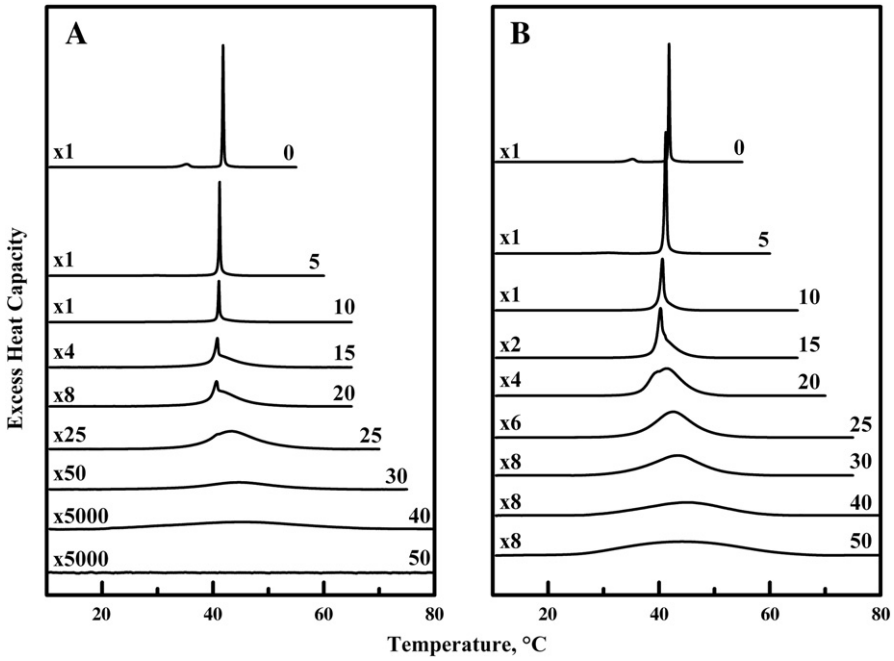

Fig. 2. DSC thermograms illustrating the effect of cholesterol (A) and ergosterol (B) on the gel/liquid-crystalline phase transition of DPPC. The thermograms shown were acquired at the sterol concentrations (mol%) indicated and have all been normalized against the mass of DPPC used. *Y*-axis scaling factors are indicated on the left hand side of each thermogram.

of ΔH (Fig. 4B) decrease more rapidly in the Erg/DPPC samples, where the pretransition is abolished at an Erg concentration of ~7 mol%, whereas it persists up to a Chol concentration of ~10 mol %. The values of $\Delta T_{1/2}$ (Fig. 4C) increase at a similar rate to those of the Chol/DPPC samples up to ~5 mol%, above which they reach a maximum which is unchanged up to 7 mol%. Since the sterol concentration at which the pretransition is abolished is less in the Erg/DPPC samples than in those containing Chol, we can conclude that Erg is more effective at abolishing the pretransition than is Chol on a molar basis.

3.2.1. The effects of sterol concentration on the main phase transition of DPPC

The DSC data shown in Fig. 2 indicate that at low to moderate sterol concentrations, both Chol- and Erg-containing DPPC bilayers exhibit asymmetric thermograms which consist of at least two

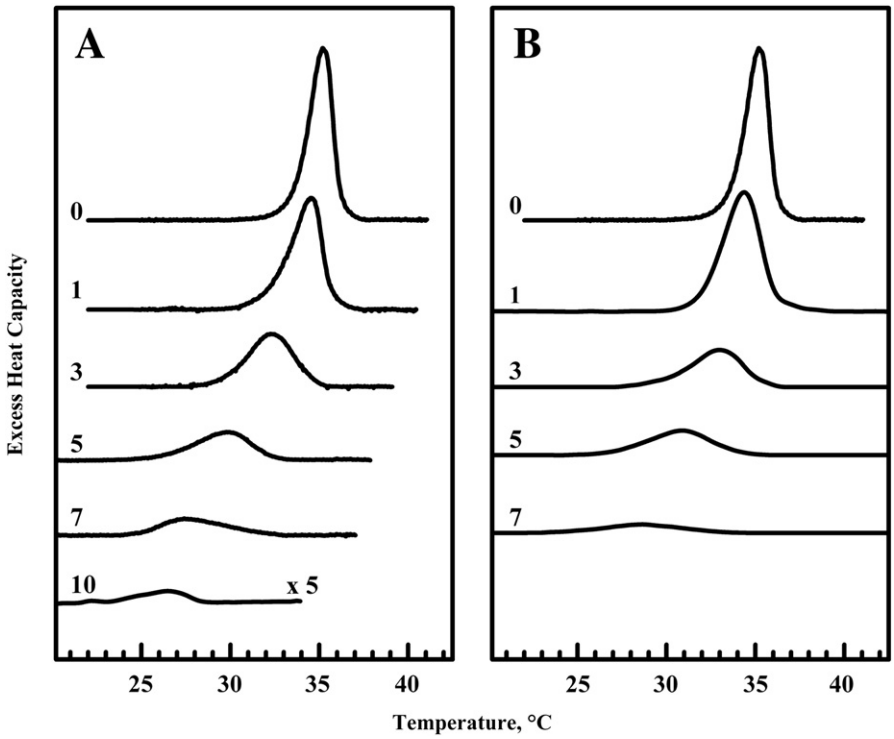

Fig. 3. DSC thermograms illustrating the effect of cholesterol (A) and ergosterol (B) on the pretransition of DPPC. The thermograms shown were acquired at the sterol concentrations (mol%) indicated and have all been normalized against the mass of DPPC used. The thermograms shown for DPPC:sterol mixtures containing 10 mol% cholesterol and 7 mol% ergosterol are plotted on 5-fold expanded y-axis relative to all others.

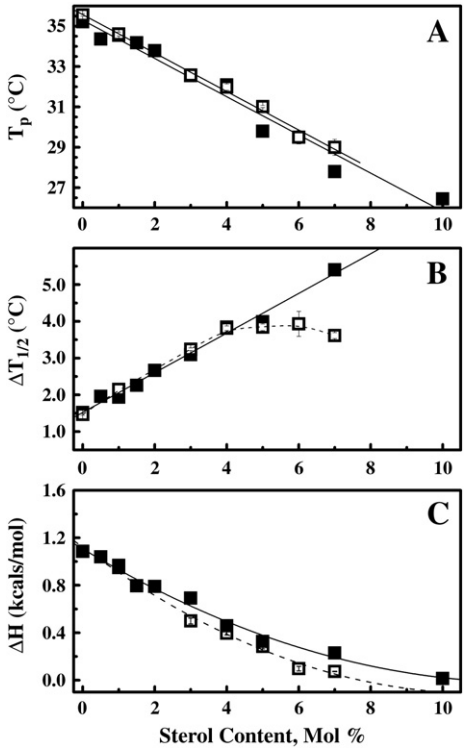

Fig. 4. The effect of increases is sterol concentration on the T_p, ΔH and $\Delta T_{½}$ of the pretransition of DPPC. The symbols (—■—■—) and (—□-—□-—) represent the data from the cholesterol- and ergosterol-containing samples, respectively.

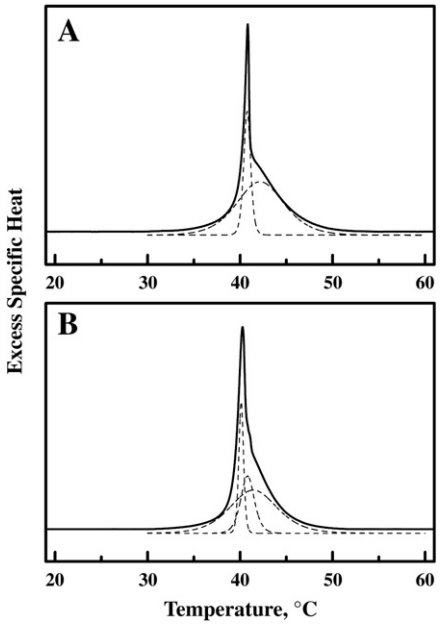

Fig. 5. Illustration of the results typically obtained in our peak-fitting deconvolution analyses of the DSC thermograns exhibited by cholesterol-containing (A) and ergosterol-containing (B) DPPC bilayers. Both thermograms are from samples containing 15 mol% sterol. To facilitate visibility, the fitted curves are slightly displaced along the y-axis.

overlapping thermal events. One of these components is considerably sharper than the others, its peak temperature and cooperativity decrease slightly, but its enthalpy decreases markedly with increasing sterol content. The other component (or components) is considerably broader, its midpoint temperature(s) exhibits a more complex dependence on sterol content, and it is the only component(s) persisting at the higher range of sterol concentrations. This pattern of sterol concentration-dependent behavior has been observed previously [32,38–43] and the resolved sharp and broad components have been ascribed to the differential melting of sterol-poor and sterol-rich lipid domains, respectively. However, there are significant differences between the sterol concentration-dependent behaviors exhibited by the Chol- and Erg-containing preparations, especially with regard to the quantitative aspects of the sterol concentration dependence of the number and overall properties of the underlying sharp and broad peaks (see Fig. 5). This aspect of our experimental observations was further examined through the application of computer-assisted curve- and peak-fitting procedures to deconvolve the observed DSC thermograms into their component peaks, so that the sterol-concentration dependence of each component could be examined and compared (see below).

The data presented in Fig. 5 are an example of the results typically obtained in our curve-fitting analyses of the DSC thermograms exhibited by the Chol- and Erg-containing mixtures. These results indicate that at lower sterol concentrations, the observed DSC thermograms of the Chol-containing mixtures can be accurately simulated by a summation of two components (one sharp and one broad), whereas those of the Erg-containing preparations can only be accurately simulated if one assumes that the DSC thermograms are summations of one sharp and at least two broad components (see Fig. 5). Moreover, we find that in the higher range of sterol concentrations, the thermograms exhibited by the Chol-containing bilayers can be accurately simulated by a single broad, low-enthalpy component above a sterol concentration of ~20 mol%, whereas simulation of the thermograms of the Erg-containing mixtures requires the assumption of at least two broad, low-enthalpy components (see Fig. 5) up to a sterol concentration of 25 mol%. These observations strongly suggest that bilayers derived from DPPC mixtures of moderate to high Erg content contain at least two significant populations of independently melting, Erg-rich domains, a possibility which is also supported by the results of our FTIR spectroscopic studies (see below). A similar pattern of behavior was also seen our earlier study of Lano/DPPC mixtures [44]. We present below a detailed analysis of the effects of variations in Chol and Erg content on the sharp and broad components seen in our DSC thermograms.

3.2.2. Effect of cholesterol and ergosterol on the sharp component of the DPPC main phase transition

The T_m values obtained from the sharp and broad components of the main phase transition of both the Chol/DPPC and Erg/DPPC mixtures are shown in Fig. 6. The sharp components of both sterol/DPPC systems (Fig. 6A) show a gradual decrease in T_m, which closely follows the T_m values obtained for the overall DSC curves. Above 5 mol%, the decrease in the T_m values of the Chol/DPPC mixtures levels off and reaches a minimum at 20 mol%, whereas that of the Erg/DPPC samples continues to decrease with increasing sterol concentration. A similar rapid linear decrease in T_m^{shp} has also been reported for some synthetic saturated isobranched sterol/PC mixtures [46,47], suggesting that there is a significant difference in the properties of the alkyl chain in Erg vs. Chol.

The corresponding values of $\Delta T_{1/2}$ for the sharp components of both sterol/DPPC mixtures (Fig. 6B) also closely follow those of the overall curve at low sterol concentrations and are virtually identical up to a concentration of 10 mol% in both sterol/DPPC systems. At higher sterol concentrations, the $\Delta T_{1/2}^{Shp}$ values of the Chol/DPPC mixtures increase gradually above 10 mol%, whereas those of the Erg/DPPC mixtures increase more slowly, reflecting the different abilities of these sterols to broaden the DPPC main phase transition.

In contrast, the pattern of ΔH values for the sharp component of both sterol/DPPC systems is more complex (Fig. 6C). After the initial drop in enthalpy, the ΔH^{shp} values for both sterol/DPPC mixtures are indistinguishable from one another up to a sterol concentration of ~3 mol%. Above 3 mol%, the ΔH^{shp} values of both sterol/DPPC

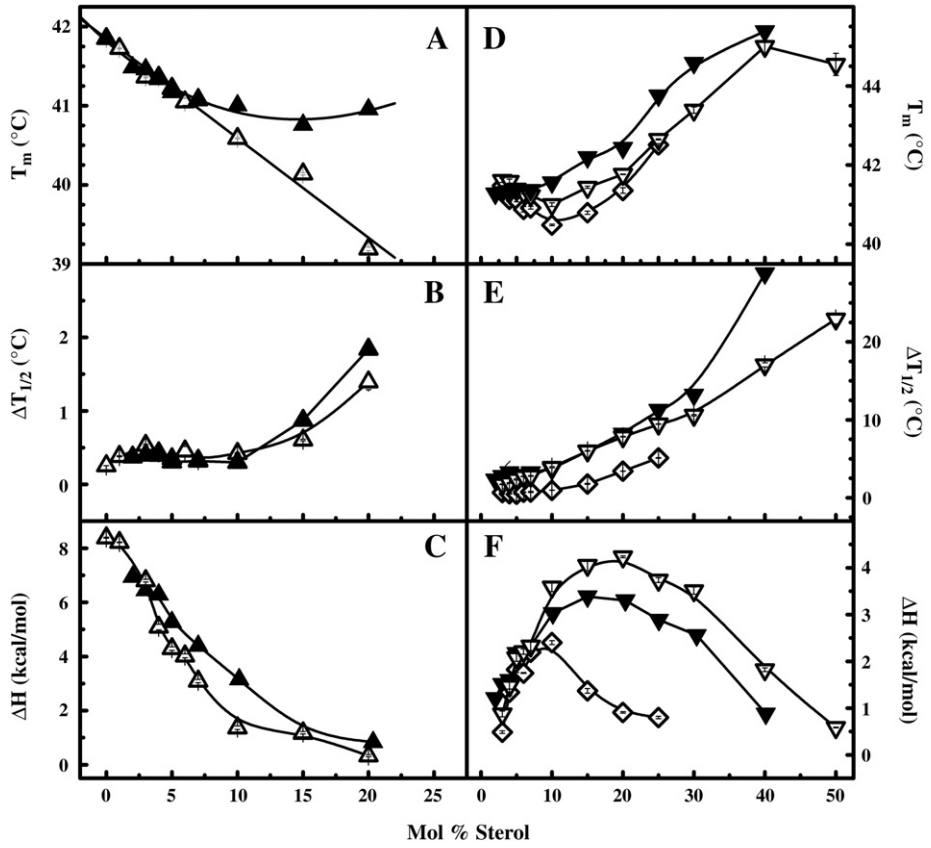

Fig. 6. Thermodynamic parameters for the deconvolved sharp (A–C) and broad (D–F) components obtained from the DSC heating thermograms of the cholesterol (▲,▼) and the ergosterol (△, ▽, ◊)/DPPC samples as a function of sterol concentration. The empty diamond represent the lower temperature broad component of the ergosterol/DPPC samples. The error bars were typically equal to, or smaller than, the size of the symbols.

mixtures continue to decrease, but those of the Erg/DPPC samples decrease more rapidly than those of samples containing Chol (Fig. 6C). Also, in both sterol /DPPC systems, the sharp component is abolished at ~20–25 mol% sterol, suggesting that the two sterols are similar in their ability to abolish the gel to liquid-crystalline phase transition of the sterol-poor domains of these binary mixtures, although subtle differences in T_m^{Shp} and $\Delta T_{1/2}^{Shp}$ remain.

3.3. Effect of cholesterol and ergosterol on the broad component(s) of the DPPC main phase transition

An analysis of the broad components obtained from our deconvolution of the overall DSC thermograms for both sterol/DPPC systems is shown in Fig. 6D–F. The broad component of the Chol/DPPC thermograms shows a linear increase in temperature over the entire range of sterol concentrations (Fig. 6D). In the Erg/DPPC mixtures, our analysis produced two broad peaks using the abovementioned deconvolution of the overall thermogram. Of those two broad components, the first, BC1 [44], is initially found on the low temperature side of the sharp component at a sterol concentration of 1–2 mol%. The second broad component, termed Erg-BC2, appears at a concentration of ~3 mol% sterol. Below a concentration of 10 mol% sterol, plots of Erg T_m^{BC1} and T_m^{BC2} overlap those of the corresponding sharp component, T_m^{shp}, with all three component parameters decreasing at similar rates, suggesting that the domains associated with Erg-BC1 and -BC2 may have similar properties and/or compositions. However, above 10 mol % sterol, the Erg T_m^{BC1} is found at a temperature below T_m^{BC2}, but both increase in temperature linearly at approximately the same rate until Erg-BC1 is abolished at a concentration of approximately 25 mol% sterol. At higher Erg concentrations, the temperature of the Erg-BC2 continues to increase linearly and reaches a maximum at a sterol concentration of 40 mol%, above which it is more difficult to accurately measure the temperature of the peak. Thus, at concentrations below 7 mol%, the phase transition temperatures of the Erg-BC1 and BC2 behave similarly to that of the broad component seen in the deconvolved Chol/DPPC system. However, at sterol concentrations above 10 mol%, both Erg-BC1 and BC2 are found at lower temperatures than that of the Chol/DPPC broad component, although the rate of temperature increase is similar for all three component temperature parameters. Again, this is reminiscent of the behavior of the broad component seen in synthetic, short-chain isobranched sterol/PC mixtures [46,47], suggesting that the Erg chain behaves differently to that of Chol in both ordered and disordered phases. These differences probably arise from differences in the miscibility and packing of Erg and Chol, where the Chol and DPPC seem to be freely miscible.

For both sterol/DPPC systems, the $\Delta T_{1/2}$ values of the broad components are significantly larger than those of the sharp component and show a gradual increase with increasing sterol concentration. In the Erg/PC system, the $\Delta T_{1/2}^{BC1}$ values are smaller than those of $\Delta T_{1/2}^{BC2}$ at all concentrations observed. Erg-BC1 seems to be abolished above a sterol concentration of 20–25 mol% , yet does not become very broad as does the Erg-BC2 component or the broad component of the Chol/DPPC system. As we previously reported [44], this may be an artifact which arises from the inability of the deconvolution routine to identify small components against a broad, highly energetic second component. The values of the Erg/DPPC $\Delta T_{1/2}^{BC2}$ increase linearly with increasing sterol concentration and, above 20 mol%, where a contribution from $\Delta T_{1/2}^{BC1}$ is essentially absent, are significantly smaller than those of the Chol/DPPC broad component, indicating that Erg does not broaden the overall DPPC phase transition to the same extent as Chol.

The ΔH values of the Chol/DPPC broad component gradually increase up to a concentration of approximately 15–20 mol%, above which they steadily decrease and the phase transition is abolished between 40 and 50 mol%. Both of the broad components of the Erg/DPPC system seem to follow a similar pattern in which they increase at low concentrations, reach a maximum and then gradually decrease with increasing sterol concentration. Up to a sterol concentration of 7 mol%, the Chol ΔH^{brd} values are very similar to those of the Erg ΔH^{BC1} and ΔH^{BC2}. Above 7 mol% sterol, the values of ΔH^{BC1} are smaller than the those of the Chol ΔH^{brd} and Erg ΔH^{BC2}, reaching a maximum at ~10 mol% and then decreasing before being abolished at ~25 mol% sterol. The values of Erg ΔH^{BC2} are higher than those of Chol ΔH^{brd} at all concentrations above 7 mol% and, at a sterol concentration of 50 mol%, there is still a poorly energetic broad peak present, indicating that Erg does not abolish the main chain-melting phase transition of DPPC as effectively as Chol. At an Erg concentration of 15 mol%, both the Erg-BC1 and –BC2 components have higher values of T_m and $\Delta T_{1/2}$. In addition, the Erg ΔH^{shp} and ΔH^{BC1} are similar, whereas the ΔH^{BC2} is significantly larger. A comparison of the all three thermodynamic parameters for both the Chol and Erg/DPPC systems (Fig. 6) shows that the Erg/DPPC sharp component is reduced slightly more rapidly than that of samples containing Chol, but, by virtue of a greater downward shift in T_m^{shp} and a smaller increase in $\Delta T_{1/2}^{shp}$, the deconvolution program is better able to resolve the broad and sharp components. Nevertheless, the fact that the sharp component parameters for the Chol/DPPC mixtures are consistently higher than those of the Erg/DPPC mixtures implies that there is a difference in the way in which Erg and Chol perturb the sharp and broad components of the DSC thermograms. This view is supported by the plot of the overall enthalpy for both sterol/DPPC systems shown in Fig. 7, which shows that the overall ΔH values are consistently higher for the Erg-containing samples above a concentration of ~7 mol% than for the corresponding samples containing Chol.

A plot of net temperature shift for both Chol- and Erg-containing samples is shown in Fig. 8. The temperature shift of the sharp component for the Erg/DPPC dispersions is significantly more negative than that of the corresponding Chol/DPPC values. Likewise with the broad components, the values obtained for the Chol-containing broad component are significantly higher than those for both the Erg-BC1 and -BC2. From Fig. 6, it is apparent that there are also significant differences in the values of the Chol T_m^{shp} (higher), $\Delta T_{1/2}^{shp}$ (higher) and ΔH^{brd} (lower) and Erg T_m^{BC2}, $\Delta T_{1/2}^{BC2}$ and ΔH^{BC2}, respectively, implying the existence of some type of enthalpy/entropy compensation process in which the sterol chemical structure, dynamics and conformation moderate the sterol/PC partition coefficient and stoichiometry, and consequently, the packing of the sterol in the DPPC bilayer.

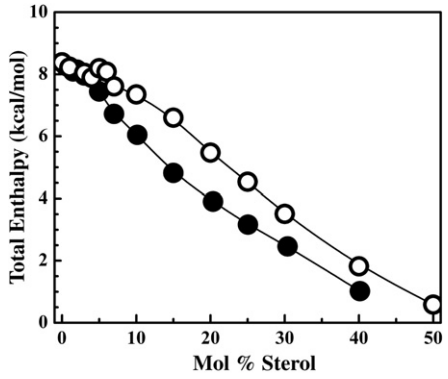

Fig. 7. Overall enthalpy values obtained for cholesterol (●) and ergosterol (○) /DPPC mixtures from DSC heating curves. The empty circles are samples containing cholesterol, whereas the filled circles are samples containing ergosterol. The largest error bar was equal to the symbol diameter.

3.4. Fourier transform infrared spectroscopic studies

The temperature-induced changes in the FTIR spectra exhibited by a sample of Erg-containing DPPC bilayers (~30 mol% sterol) over the temperature range 0–60 °C are illustrated in Fig. 9. These data exhibit several features that are common to the sterol-free and sterol-containing bilayers examined here. First, the dominant features of the C-H stretching region (3000–2800 cm^{-1}) are absorption bands centered near 2849–2852 cm^{-1} and 2916–2922 cm^{-1} (see Fig. 9A). These bands arise from the symmetric and asymmetric C–H stretching vibrations of CH_2 groups, respectively, and are sensitive to the conformational disposition of the hydrocarbon chains of the lipids [48–50]. At temperatures below the onset of the lipid hydrocarbon chain-melting phase transition, these bands are relatively sharp and centered at lower frequency, indicating the predominance of relatively immobile hydrocarbon chains in the all-*trans* conformation [48–50]. Upon heating to temperatures above the hydrocarbon chain-melting phase transition, these bands broaden and their peak frequencies increase by values ranging from ~1.5–3 cm^{-1} (CH_2 symmetric C-H stretch) to ~2–5 cm^{-1} (CH_2 asymmetric stretch), changes consistent with the increased mobility of the vibrating groups and with the increase in the *gauche* rotamer content (or conformal disorder) of the hydrocarbon chains. Second, the dominant feature of the region between 1800 and 1650 cm^{-1} is a broad absorption band envelope which arises from the stretching vibrations of ester C═O groups located in the bilayer polar/apolar interface. Typically, this band envelope is resolvable into subcomponents which are usually centered at frequencies near 1743 cm^{-1} and 1728 cm^{-1}, respectively [48–50], and have been assigned to the stretching vibrations of populations of free and H-bonded ester carbonyl groups (for examples, see Fig. 11). The changes in the shape of the C═O stretching absorption band which accompany the gel/liquid-crystalline phase transitions of these lipids are usually the result of changes in the relative intensities of these subpopulations, reflecting changes in the hydration and/or the number or strength of hydrogen-bonding interactions involving the ester carbonyl groups in the interfacial region [48,50 and references cited therein]. Finally, Fig. 9C shows that the main feature of the C-H deformation region between 1500 and 1400 cm^{-1} is an absorption band centered near 1465–1472 cm^{-1}, which arises from the scissoring vibrations of the lipid methylene groups [48,50 and references cited therein]. These bands are sensitive to lateral packing interactions between lipid hydrocarbon chains, and can thus provide information on the perturbation of the hydrocarbon chain subcell packing and the ordering of domains present, especially at lower temperatures where all-*trans* lipid hydrocarbon chains predominate. The relative effects of Chol and Erg on thermally-induced changes in the C-H stretching, C═O stretching and CH_2 scissoring vibrations of DPPC bilayers are examined in more detail below.

The top panel of Fig. 10 shows a comparison of the temperature-induced changes in the frequencies of the CH_2 symmetric stretching bands exhibited by pure DPPC bilayers and by DPPC bilayers containing 30 mol% Chol or Erg. A plot of the frequency of the CH_2 symmetric stretching bands of pure DPPC bilayers exhibits a sharp increase in frequency at temperatures centered near 42 °C (Fig. 10), indicating the occurrence of a highly cooperative hydrocarbon chain-melting phase transition. In contrast, the corresponding temperature-induced changes in the frequency of the CH_2 symmetric stretching band exhibited by the Chol- and Erg-containing DPPC bilayers span a considerably broader temperature range, consistent with the broader hydrocarbon chain-melting phase transitions exhibited by the sterol-containing samples obtained by DSC (see Figs. 2 and 10). The nature of the changes occurring with the Chol-containing sample has been described fully in previous publications from this laboratory [39,44] and will not be detailed here. However, the curve describing the changes in the CH_2 symmetric stretching frequency of the Erg-

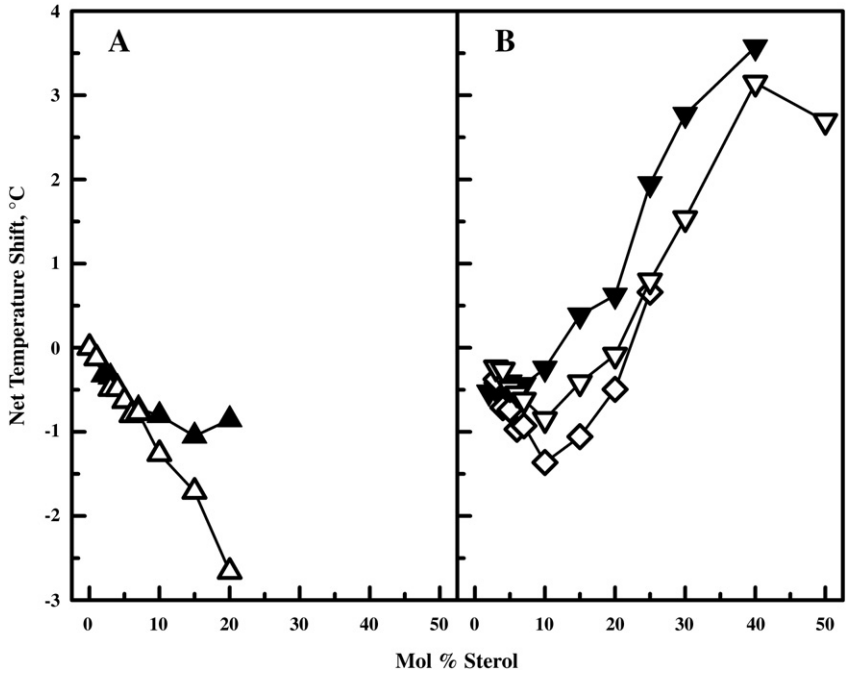

Fig. 8. The net temperature shift of the sharp and broad components of the main chain melting phase transition of cholesterol (▲,▼) and ergosterol/DPPC (△, ▽, ◊) samples obtained from DSC heating thermograms relative to that of pure DPPC. Two broad components exist in the ergosterol samples which are depicted here as either an empty inverted triangle (upper temperature component) or an empty diamond (lower temperature component).

containing sample spans a broader temperature range than does that of the Chol-containing sample. Moreover, the upward drift in CH_2 symmetric stretching frequency begins at lower temperatures and the temperature range spanned seems to be even broader than observed by DSC (see Fig. 2). However, an examination of the DSC thermograms exhibited by the Erg-containing DPPC sample on a highly expanded heat capacity scale indicates that the temperature range spanned by

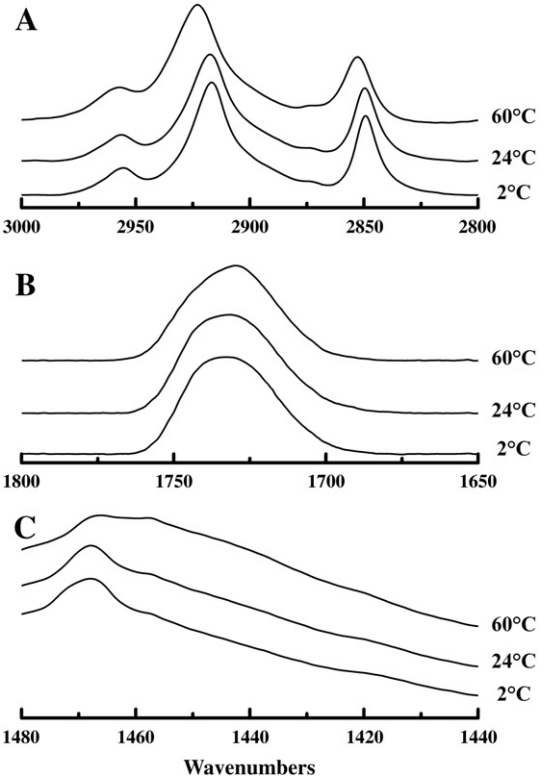

Fig. 9. Representative spectra illustrating the temperature-dependent changes in the contours of the FTIR spectra of ergosterol-containing DPPC bilayers. The data shown were acquired at the temperatures indicated with a DPPC-ergosterol mixture containing ~30 mol% ergosterol and typify the changes in the band contours observed in the C-H stretching (A) and the C═O stretching (B) and CH_2 scissoring (C) regions of the infrared spectrum.

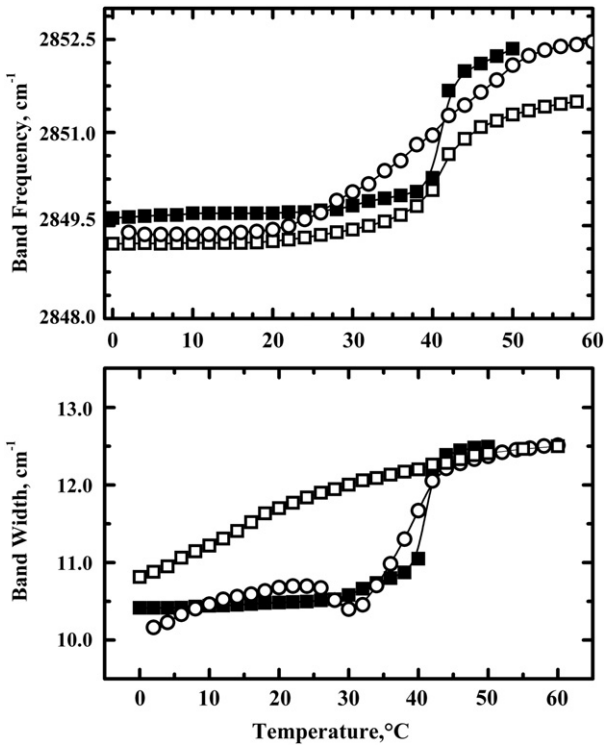

Fig. 10. Temperature-dependent changes of the properties of the CH_2 symmetric stretching band exhibited by sterol-free DPPC bilayers (— ■—), and by DPPC bilayers containing ~30 mol% cholesterol (—□ —) and ~30 mol% ergosterol (— ○—). The data shown were obtained by analyses of spectra acquired in the heating mode with the top panel illustrating the temperature-induced changes in the band maxima and the bottom panel showing the corresponding changes in overall band width.

their heat capacity integrals is actually similar to the thermally induced changes in CH_2 symmetric stretching frequency (data not shown). This pattern was also observed with all of the Erg-rich DPPC preparations examined. These observations suggest that aside from the main hydrocarbon chain-melting process, there may be other processes occurring in Erg-rich DPPC bilayers which significantly alter the time-averaged conformation of the hydrocarbon chains, while making relatively small contributions the overall heat capacity changes involved.

The bottom panel of Fig. 10 shows a comparison of the temperature-dependent changes in the CH_2 symmetric stretching bandwidths exhibited by sterol-free and by Chol- and Erg-containing DPPC bilayers. Changes in CH_2 stretching bandwidths are useful monitors of changes in hydrocarbon chain mobility [48–50]. With pure DPPC bilayers, small monotonic increases in CH_2 symmetric stretching band widths are observed at low temperatures, consistent with the thermally induced increases in the mobility of the vibrating groups (Fig. 10, bottom panel). The data also show that a discontinuous increase in CH_2 symmetric stretching bandwidth occurs at temperatures near 35 °C and that a considerably larger increase in bandwidth occurs at temperatures near 42 °C. These temperatures correlate strongly with calorimetric endotherms arising from the well-characterized pretransition and gel/liquid-crystalline phase transition of DPPC, and the magnitude of the increases in CH_2 symmetric stretching bandwidths observed are also consistent with the relative increases in hydrocarbon chain mobility which occurs at these two thermotropic phase transitions [48–50]. In the case of the Chol-rich DPPC bilayers, small continuous increases in CH_2 symmetric stretching bandwidth are observed over the entire temperature range examined (Fig. 10, bottom panel). This pattern of behavior is generally compatible with the occurrence of a single broad thermotropic event, consistent with our calorimetric observations. In the case of the Erg-rich DPPC bilayers, small monotonic changes in bandwidths are also observed at low temperatures (Fig. 10, bottom panel). However, at temperatures near 25–30 °C, there is a major discontinuity in the temperature dependence of the CH_2 symmetric stretching bandwidths, in which a decrease in CH_2 symmetric stretching bandwidth occurs prior to the onset of a relatively large increase in bandwidth at temperatures above 30 °C. Interestingly, the relatively large increase in CH_2 symmetric stretching bandwidth spans a temperature range compatible with that of the broad endothermic transition resolved by DSC. This suggests that the main structural changes leading to an increase hydrocarbon chain mobility in the Erg-containing bilayers (i.e., hydrocarbon chain-melting) actually occur at temperatures above 30 °C, and that the structural changes occurring at temperatures below 30 °C are probably different from the hydrocarbon chain-melting process.

As noted above, the ester C═O stretching bands exhibited by both sterol-free and sterol-containing DPPC bilayers consists of a broad envelope that is a summation of subcomponents. The panels A and B in Fig. 11 show results which exemplify our component analysis of the sterol-free DPPC bilayers which, aside from variations in the widths and integrated intensities of the component bands, also typify our analyses of the Chol-containing bilayers. Our analyses of the sterol-free and Chol-containing DPPC samples indicate that the C═O stretching band envelopes of both preparations are all resolvable into subcomponents centered near 1728 cm^{-1} and 1743 cm^{-1}, and as illustrated in Table 1, the effects of changes in temperature, phase state and Chol content are reflected primarily by changes in the widths and integrated intensities of the component bands, without significant changes in their frequencies, as noted in previous studies [44,51–52]. The results summarized in Table 1 also indicate that with both the sterol-free and Chol-containing bilayers, the transition from their low-temperature to high-temperature phases is accompanied by an increase in the relative intensities of the lower-frequency band, suggesting that the process is accompanied by an increase in the size of the hydrated or hydrogen-bonded population of ester carbonyls at the expense of the free ester carbonyl groups.

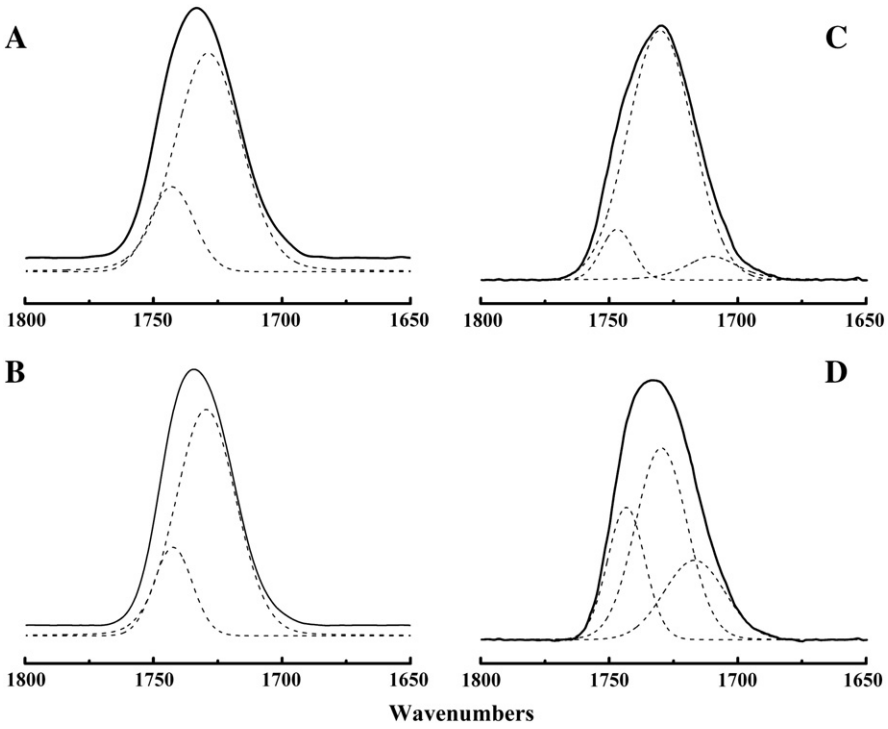

Fig. 11. Component analysis of the ester carbonyl absorption bands observed in sterol-free and sterol-containing (~30 mol%) DPPC bilayers at temperatures above (top) and well below (bottom) their hydrocarbon chain-melting phase transitions. Panels A and B show data obtained in our analyses of DPPC pure bilayers which, aside from variations in the widths and integrated intensities of the components, also typify our analyses of the cholesterol-containing bilayers. Panels C and D show typical component analyses of the ergosterol-containing DPPC bilayers. Note the additional low-frequency component between 1710 and 1715 cm^{-1}.

Table 1
Characterization of the subcomponents of the ester C═O stretching bands exhibited by hydrated sterol-free and sterol-containing DPPC bilayers[a].

A. DPPC (Lβ phase at 6 °C)		
Peak maximum (cm^{-1})	Peak width (cm^{-1})	Peak area (% total)
1728	27	76
1742	17	24
B. DPPC (L_α phase at 60 °C)		
Peak maximum (cm^{-1})	Peak width (cm^{-1})	Peak area (% total)
1728	30	82
1742	19	18
C. DPPC + 30 mol% cholesterol (solid-disordered phase at 6 °C)		
Peak maximum (cm^{-1})	Peak width (cm^{-1})	Peak area (% total)
1728	30	80
1742	19	20
D. DPPC + 30 mol% cholesterol (liquid-ordered phase at 60 °C)		
Peak maximum (cm^{-1})	Peak width (cm^{-1})	Peak Area (% total)
1728	33	84
1742	20	16
E. DPPC + 30 mol% Ergosterol (Solid-disordered Phase at 6 °C)		
Peak maximum (cm^{-1})	Peak width (cm^{-1})	Peak area (% total)
1716	27	25
1729	23	50
1743	15	25
F. DPPC + 30 mol% Ergosterol (Liquid-ordered Phase at 60 °C)		
Peak maximum (cm^{-1})	Peak width (cm^{-1})	Peak area (% total)
1710	23	7
1730	29	85
1745	17	8

[a] Parameter values are all rounded to the nearest whole number.

Fig. 11 also shows that the contours of the C═O stretching band envelope of Erg-rich DPPC bilayers (panels C and D) differ markedly from those which typify the sterol-free and Chol-rich preparations (see panels A and B). Specifically, the C═O stretching band envelope exhibited by the Erg-rich bilayers are better described by a summation of three subcomponents, centered near 1710–1715 cm^{-1}, 1728–1730 cm^{-1} and 1743 cm^{-1}. The appearance of an additional low-frequency ester carbonyl subcomponent suggests that Erg-rich DPPC bilayers contain a population of hydrogen-bonded ester carbonyl groups that is not present in either the sterol-free or Chol-containing DPPC bilayers. With these Erg-rich bilayers, the conversion from the low- to the high-temperature state is also accompanied by an increase in the relative size of the H-bonded populations of ester C═O groups (see Table 1). However, in this case the process involves significant increases in the relative areas of the 1728–1730 cm^{-1} component at the expense of the both the higher- and lower-frequency components centered near 1743–1745 cm^{-1} and 1710–1715 cm^{-1}, respectively, suggesting that the emergence of the lower-frequency population near 1710–1715 cm^{-1} is thermodynamically favored at low temperatures.

The left panel in Fig. 12 shows a stacked plot illustrating the temperature-dependent changes in the contours of the CH_2 scissoring bands arising from hydrocarbon chain methylene groups in a sample of Erg-containing DPPC bilayers (~30 mol% sterol). At low temperatures, the main absorption band near 1465 cm^{-1} consists of a relatively broad asymmetric band envelope that is resolvable into components centered near 1472 and 1466 cm^{-1} (marked by asterisks in Fig. 12). This observation is a manifestation of the so-called factor group splitting of the CH_2 scissoring band, the result of inter-chain coupling of the scissoring vibrations of methylene groups on all-*trans* polymethylene chains packed in an orthorhombic ⊥ subcell (see 48, 50 and references cited therein). Its occurrence in the low-temperature FTIR spectra of the Erg-containing sample thus indicates that the DPPC-Erg bilayers contain extended arrays of close packed

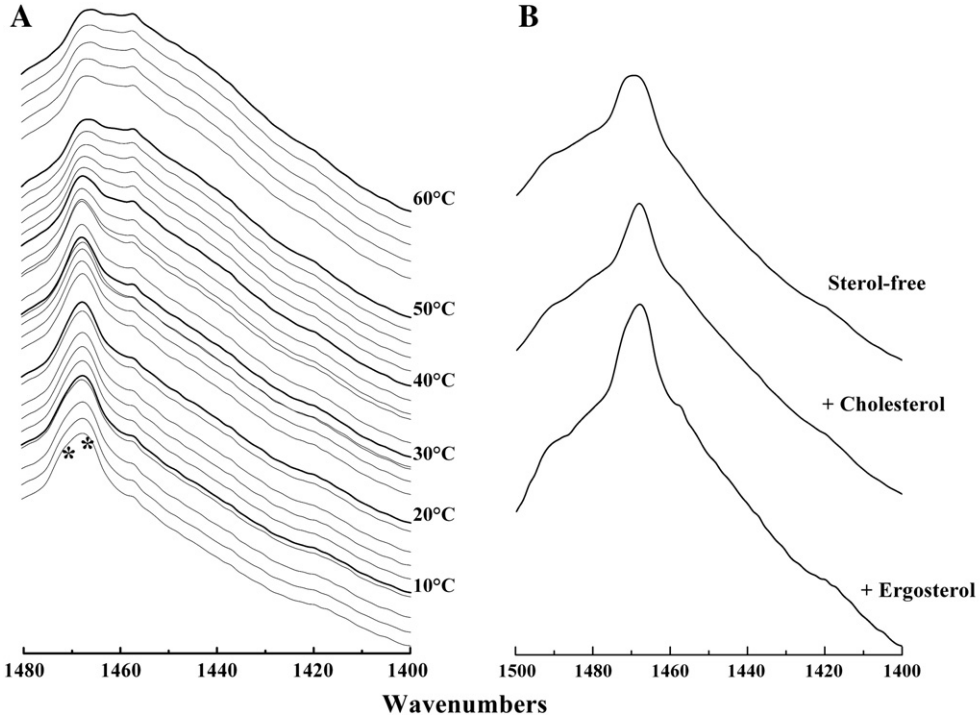

Fig. 12. Temperature-dependent changes in the CH_2 scissoring bands of sterol-free and sterol-containing DPPC bilayers. Panel A shows a stacked plot of the CH_2 scissoring region of the FTIR spectra exhibited by ergosterol-containing DPPC bilayers. The spectra were acquired at the temperatures indicated and the asterisks indicate the positions of the component bands arising from the factor group splitting of the main methylene scissoring band at low temperature. Panel B shows a comparison the contours of the CH_2 scissoring bands observed in the FTIR spectra of sterol-free, cholesterol-containing and ergosterol-containing (~30 mol%) DPPC bilayers at temperatures near 0 °C. Note that factor group splitting is observed with the sterol-free and ergosterol-containing bilayers but not with the cholesterol-containing bilayers.

all-*trans* hydrocarbon chains at low temperatures. Upon heating, the magnitude of the factor group splitting gradually diminishes and effectively collapses at temperatures near 20 °C, such that a single symmetrical band is observed at frequencies near 1467 cm^{-1}. Upon further heating to temperatures near to and above the hydrocarbon chain-melting phase transition temperature of the sample, this band broadens considerably. The latter spectroscopic changes are observed with the sterol-free and with the sterol-containing preparations and are consistent with the increased mobility of the methylene groups which occurs at lipid hydrocarbon chain-melting phase transitions. However, the thermally induced collapse of factor-group splitting observed at temperatures well below the onset of the hydrocarbon chain-melting phase transition is of special significance to this work, because it is indicative of a thermally induced weakening of lateral interactions between hydrocarbon chains. In hydrocarbon chain-homogeneous systems (e.g. pure DPPC), that process is entirely attributable to thermally induced increases in the rates and amplitudes of the reorientational fluctuations of the hydrocarbon chains. However, with the sterol-containing bilayers, there are also other potential contributory factors, the nature and significance of which will be examined later. However, we note that the low-temperature factor-group splitting is not observed with the Chol-containing system, and that it is more pronounced in pure DPPC bilayers than in the Erg-rich mixtures (Fig. 12, panel B). These observations suggest that the incorporation of ~30 mol% Chol or Erg into DPPC bilayers inhibits the formation of extended domains of laterally-interacting, all-*trans* hydrocarbon chains at low temperatures. The data also suggest that although the formation of such domains is only attenuated by such quantities of Erg, it is essentially completely inhibited by the presence of comparable amounts of Chol. Given this and the fact that the formation of sterol-poor DPPC domains within sterol-rich DPPC bilayers requires some degree of sterol-DPPC demixing, it follows that the DPPC/Erg-mixture must be more prone to low-temperature induced demixing than the corresponding Chol/DPPC mixture. The suggestion that Erg-rich DPPC bilayers may be more prone to low temperature-induced sterol-phospholipid demixing than its Chol-rich counterpart has important implications regarding the relative miscibilities of Chol and Erg in DPPC bilayers.

4. Discussion

The preferred conformations of Chol and Erg are shown qualitatively in Fig. 1C–E [11]. Although the alkyl side of Chol in much more conformationally flexible than in Erg, the lowest energy conformation of Chol is characterized by a fully extended, *all-trans* isooctyl side, resulting in a sterol molecule in which the alkyl side chain and steroid ring system are essentially coplanar (see Fig. 1C). In contrast, due to the lack of free rotation about the *trans* double bond between C_{22}–C_{23} of the alkyl chain and the presence of methyl groups at C_{21} and C_{24}, free rotation about the C_{21}–C_{22} and C_{23}–C_{24} carbon–carbon single bonds is markedly restricted, especially in the former case. Due to the restricted flexibility of this segment of the alkyl side chain, there exist two dominant conformers of Erg, which are separated by a markedly energetic barrier for interconversion. In the slightly dominant conformer, the alkyl side chain is largely extended, but is slightly bent relative to the mid-plane steroid ring system (Fig. 1D), while in the other major conformer, the alkyl chain is less extended and forms a sharper angle with the steroid ring system. Note that the effective cross-sectional areas of the two Erg conformers are larger than that of the dominant Chol conformer, and that the effective lengths of the Erg conformers are considerably less than that of the major Chol conformer. We believe that a consideration of the structure of the dominant conformers of Chol and Erg can explain many of our experimental findings and some of those in the previous literature.

The effect of Chol and Erg on the thermotropic phase behavior of DPPC bilayers differ quantitatively at lower sterol concentrations, and both qualitatively and quantitatively at higher sterol concentrations, despite their rather similar chemical structures. In particular, Erg reduces both the enthalpy and the cooperativity of the pretransition of DPPC with increasing sterol concentration more markedly than does Chol. As a result, the DPPC pretransition is abolished entirely at a Erg concentration of only ~7 mol% sterol whereas the pretransition persists until 10 mol% sterol in Chol/DPPC mixtures. We postulate that the presence of the Erg conformers with less than fully extended alkyl chains, which are bent relative to the plane of the steroid ring system, will occupy a larger cross-sectional area than Chol and will thus also be more effective at relieving the cross-sectional area mismatch between the larger polar headgroups and the smaller hydrocarbon chains in a gel state DPPC, as observed. Moreover, the shorter effective hydrophobic length of the Erg conformers will also produce more disorder in the gel state DPPC hydrocarbon chains, due to a greater degree of hydrophobic mismatch between the sterol molecule and phospholipid all-*trans* hydrocarbon chains, further augmenting its effect in abolishing the pretransition relative to Chol.

Erg also has a similar effect on the sharp component of the DSC endotherm, reducing the temperature, enthalpy and cooperativity of this component more rapidly than does Chol. Thus, the sharp component of the DSC endotherm is abolished at an Erg concentration in the DPPC bilayer of only about 15 mol% sterol, whereas the sharp component of the DSC endotherms persists to ~22 mol% in Chol/DPPC binary mixtures. Since the sharp components of the DSC endotherm arise from the fairly cooperative hydrocarbon chain melting of domains highly enriched in DPPC and depleted of sterol, this result could be explained by a greater perturbation by Erg relative to Chol of the gel-state organization of these DPPC-enriched domains, by a decrease in the size of these domains, or by a combination of both factors due to the effects discussed above for the pretransition. Again, these effects could be explained by the bent conformations of Erg, which may produce a greater effective size and shorter hydrophobic length than Chol. In this regard, it is interesting to note that the concentration of Erg required to abolish both the pretransition and the sharp component of the main phase transition is roughly two thirds of the concentration of Chol required to produce these effects.

The effects of the incorporation of Erg and Chol on the broad component of the DSC heating runs, which arise from the less cooperative chain melting of domains of DPPC enriched in sterol, are also somewhat different, particularly at higher sterol concentrations. In the Chol/DPPC mixtures, the temperature of the broad component monotonically increases with increasing sterol concentration while the enthalpy and cooperativity decrease, such that no cooperative phase transition can be detected at 50 mol% sterol. Although a similar qualitative effect is noted with Erg at lower sterol concentrations, there appear to be two overlapping broad components in the DSC endotherms between sterol concentrations of 3 and 10 mol%, with one component being shifted upward and the second component being shifted downward with increasing Erg levels. The higher-temperature broad component is the narrower and more energetic of the two and can even be resolved by DSC in mixtures containing 50 mol% Erg. In contrast, the lower-temperature component is broader and considerably less energetic and thus more difficult to resolve in the DSC thermograms obtained with Erg-rich DPPC samples. For such preparations, the broad lower-temperature event was more easily detected by FTIR spectroscopy and its persistence at higher Erg concentrations was consistent with the results of a more detailed derivative analysis of the DSC thermograms. Our FTIR spectroscopic studies also indicate that although conformational disordering of hydrocarbon chains occurs at both of these broad thermotropic events, it occurs predominantly at the higher-temperature event, suggesting that the hydrocarbon chain-melting process occurs largely at higher temperatures. The fact that this broad chain-melting

endotherm can still be observed at 50 mol% Erg, but not at 50 mol% Chol, also suggests that in contrast to Chol, Erg may not be fully miscible with gel state DPPC bilayers at sterol concentrations of 30 mol% and higher. In this respect, our calorimetric data are consistent with the NMR spectroscopic evidence for the existence of two separate phases in Erg-containing DMPC or DOPC bilayers at sterol concentrations in excess of 30 mol% and the existence of only a single phase in the corresponding Chol-containing vesicles [24]. However, unlike the case for Lano/DPPC bilayers [44], we do not observe any endotherms attributable to the melting or other transformations of crystalline Erg, suggesting that despite its low miscibility with DPPC, discrete domains of crystalline forms of Erg do not form under our conditions. Again, all of these observations could be explained by the existence of only partially extended and bent conformers in Erg, which would tend to pack less well in gel state DPPC bilayers and which would have a reduced tendency for crystallization in fluid DPPC bilayers.

The observation that the DSC thermograms exhibited by Erg-rich DPPC bilayers exhibit a broad, low-temperature endothermic event which is not present in DSC thermograms exhibited by comparable Chol-rich bilayers, underscores a significant difference between the effects of the two sterols. Our FTIR spectroscopic data suggest that this may be attributable to the occurrence of thermally induced structural changes within Erg-rich DPPC which are distinct from the hydrocarbon chain-melting process. These processes occur at temperatures below the onset of the main hydrocarbon chain-melting process, are very broad and weakly energetic, and are associated with increases in hydrocarbon chain mobility and conformational disorder and with the loss of lateral close contacts between all-*trans* polymethylene chains. This combination of characteristics suggests that the underlying process is a solid-phase transformation accompanied by only a small conformational disordering of the lipid hydrocarbon chains. However, our FTIR spectroscopic data also indicate that this process does not involve a major reorganization of the bilayer polar/apolar interface, suggesting that processes involving lamellar crystalline phases can be excluded. Given this and the FTIR spectroscopic evidence for the formation of Erg-poor DPPC domains at low temperature (see data presented in Fig. 12), we suggest that the broad, weakly energetic process occurring at low temperatures could be attributable to reversible solid-phase mixing/demixing of Erg with DPPC. This suggestion, and the fact that comparable processes are not observed in the corresponding Chol-rich DPPC bilayers, is consistent with the lower miscibility of Erg with DPPC, as suggested by the data presented here and elsewhere [24].

Our FTIR spectroscopic data also showed that the patterns of hydration and/or hydrogen-bonding interactions in the polar/apolar interfaces of Erg-rich DPPC bilayers differ significantly from those characteristic of either sterol-free or Chol-rich DPPC bilayers. Specifically, the polar/apolar interfaces of Erg-rich DPPC bilayers contain a population of hydrogen-bonded ester carbonyl groups that is not present in the polar/apolar interfaces of either the sterol-free or Chol-rich DPPC bilayers. With fully hydrated PC bilayers, interfacial water is the only source of donor groups available for hydrogen-bonding to the ester carbonyl groups and as a result, assignment of the H-bonded population of ester carbonyls can be relatively straightforward and unambiguous. However, with the sterol-rich PC bilayers, such assignments are complicated by the fact that the sterol hydroxyl groups are themselves potential sources hydrogen-bonding donor groups. In the case of the Chol-rich PC bilayers, the frequencies and general properties of absorption bands from the subpopulations of ester carbonyl groups (aside from the relative intensities), are very similar to those resolved in the IR spectra of pure PC bilayers (see Fig. 11), suggesting that the patterns of hydrogen-bonding to ester carbonyls in Chol-rich PC bilayers are comparable to those existing in the sterol-free bilayers. The latter also implies that H-bonding between Chol hydroxyl groups and PC ester carbonyl groups does not contribute significantly to the populations of ester carbonyl groups resolved in the IR spectra of hydrated, Chol-rich PC bilayers. In the case of the Erg-rich PC bilayers, our data suggest that Erg-rich DPPC bilayers contain an additional population of H-bonded ester carbonyl groups that are not present in either the sterol-free or Chol-rich DPPC bilayers. This population resonates at a lower frequency (~1710–1715 cm^{-1}) than that assigned to the hydrogen-bonded population typical of sterol-free and/or Chol-rich DPPC bilayers (~1725–1730 cm^{-1}), suggesting stronger interactions with its H-bonding donor groups. The presence of this additional population of H-bonded ester carbonyl groups in the Erg-rich DPPC bilayers suggests that sterol H-bonding to DPPC ester carbonyl groups is more prevalent in such bilayers than in comparable Chol-rich bilayers. This suggestion is also consistent with the fact that the additional population of ester C═O groups is more thermodynamically favored at lower temperatures.

Acknowledgements

This work was supported by operating and major equipment grants from the Canadian Institutes of Health Research and by major equipment grants from the Alberta Heritage Foundation for Medical Research. DAM would like to thank Dr. Olga Dmitrenko, University of Delaware, for useful discussions.

References

[1] W.R. Nes, M.L. McKean, Biochemistry of Steroids and Other Isopentenoids, University Park Press, Baltimore, Maryland, 1977.
[2] P.L. Yeagle, Cholesterol and the cell membrane, in: P.L. Yeagle (Ed.), The Biology of Cholesterol, CRC Press, Inc., Boca Raton, FL, 1988.
[3] L. Liscum, N.J. Munn, Intracellular cholesterol transport, Biochim. Biophys. Acta 1438 (1999) 19–37.
[4] R.A. Demel, B. de Kruijff, The function of sterols in membranes, Biochim. Biophys. Acta 457 (1976) 109–132.
[5] M.R. Vist, J.H. Davis, Phase equilibria of cholesterol/DPPC mixtures: ^{2}H-nuclear magnetic resonance and differential scanning calorimetry, Biochemistry 29 (1990) 451–464.
[6] L. Finegold (Ed.), Cholesterol in Model Membranes, CRC Press Inc., Boca Raton, FL, 1993.
[7] T.P.W. McMullen, R.N. McElhaney, Physical studies of cholesterol-phospholipid interactions, Current Opin. Colloid Interface Sci. 1 (1996) 83–90.
[8] J.H. Ipsen, G. Karlstrom, O.G. Mouritsen, H.W. Wennerstrom, M. Zuckermann, Phase equilibria in the phosphatidylcholine-cholesterol system, Biochim. Biophys. Acta 905 (1987) 162–172.
[9] J.L. Thewalt, M. Bloom, Phosphatidylcholine:cholesterol phase diagrams, Biophys. J. 63 (1992) 1176–1181.
[10] Mannock, D.A., R.N.A.H. Lewis, T.P.W. McMullen and R.N. McElhaney. The effect of variations in phospholipid and sterol structure on the nature of lipid-sterol interactions in lipid bilayer model membranes. *Chem. Phys. Lipids* (In press.)
[11] M. Baginski, A. Tempczyk, E. Borowski, Comparative conformational analysis of cholesterol and ergosterol, Eur. J. Biophys. 17 (1989) 159–166.
[12] J. Czub, M. Baginski, Comparative molecular dynamics study of lipid membranes containing cholesterol and ergosterol, Biophys. J. 90 (2006) 2368–2382.
[13] Z. Cournia, G.M. Ullmann, J.C. Smith, Differential effects of cholesterol, ergosterol and lanosterol on a dipalmitoyl phosphatidylcholine membrane: a molecular dynamics simulation study, J. Phys. Chem. B 111 (2007) 1786–1801.
[14] A.M. Smondyrev, M.L. Berkowitz, Molecular dynamics simulation of the structure of dimyristoylphosphatidylcholine bilayers with cholesterol, ergosterol, and lanosterol, Biophys. J. 80 (2001) 1649–1658.
[15] E. Endress, H. Heller, H. Casalta, M.F. Brown, T.M. Bayerl, Anisotropic motion and molecular dynamics of cholesterol, lanosterol and ergosterol in lecithin bilayers studied by quasi-elastic neutron scattering, Biochemistry 41 (2002) 13078–13086.
[16] O. Soubias, F. Jolibois, S. Massou, A. Milton, V. Real, Determination of the orientation and dynamics of ergosterol in model membranes using uniform ^{13}C labeling and dynamically averaged ^{13}C chemical shift anisotrophies as experimental restraints, Biophys. J. 89 (2005) 1120–1131.
[17] D. Ghosh, J. Tincoco, Monolayer interactions of individual lecithins with natural sterols, Biochim. Biophys. Acta. 266 (1972) 41–49.
[18] R.A. Demel, K.R. Bruckdorfer, L.L.M. van Deenen, The effect of sterol structure on the permeability of liposomes to glucose, glycerol and Rb, Biochim. Biophys. Acta 225 (1972) 321–330.
[19] I. Schuler, G. Duportail, N. Glasser, P. Benveniste, M.A. Hartmann, Soybean phosphatidylcholine vesicles containing plant sterols: a fluorescence anisotropy study, Biochem. Biophys. Acta 1028 (1990) 82–88.
[20] R. Semer, E. Gelerinter, A spin label study of the effects of sterols on egg lecithin bilayers, Chem. Phys. Lipids 23 (1979) 201–211.

[21] S. Shrivastara, A. Chattopadhyay, Influence of cholesterol and ergosterol on membrane dynamics using different fluorescent reporter probes, Biochem. Biophys. Res. Commun. 356 (2007) 705–710.
[22] C. Bernsdorff, R. Winter, Differential properties of the sterols cholesterol, ergosterol, β-sitosterol, trans-7-dehydrosterol, stigmasterol and lanosterol on DPPC bilayer order, J. Phys. Chem. B 107 (2003) 10658–10664.
[23] A. Arora, H. Raghuraman, A. Chattopadhyay, Influence of cholesterol and ergosterol on membrane dynamics: a fluorescence approach, Biochem. Biophys. Res. Commun. 318 (2004) 920–926.
[24] J.A. Urbina, S. Pekerar, H.B. Lee, J. Patterson, B. Montez, E. Oldfield, Molecular order and dynamics of phosphatidylcholine bilayer membranes in the presence of cholesterol, ergosterol and lanosterol: a comparative study using ^{2}H-, ^{13}C- and ^{31}P-NMR spectroscopy, Biochim. Biophys. Acta 1238 (1995) 163–176.
[25] J.A. Urbana, B. Moreno, W. Arnold, D.H. Taron, P. Orlean, E. Oldfield, A carbon-13 nuclear magnetic resonance spectroscopic study of inter-proton pair order parameters: a new approach to study order and dynamics in phospholipid membrane systems, Biophys. J. 75 (1998) 1372–1838.
[26] Y.-W. Hsueh, K. Gilbert, C. Trandum, M. Zuckermann, J. Thewalt, The effect of ergosterol on dipalmitoylphosphatidylcholine bilayers: a deuterium NMR and calorimetic study, Biophys. J. 88 (2005) 1799–1808.
[27] I. Fournier, J. Barwicz, M. Auger, P. Tancrede, The chain conformational order of ergosterol- or cholesterol- containing DPPC bilayers as modulated by Amphotericin B: a FTIR study, Chem. Phys. Lipids 151 (2008) 41–50.
[28] E. Endress, S. Bayerl, K. Prechtel, C. Maier, R. Merkel, T.M. Bayerl, The effect of cholesterol, lanosterol and ergosterol on lecithin bilayer mechanical properties: a solid-state NMR and micropipet study, Langmuir 18 (2002) 3293–3299.
[29] J. Henrikson, A.C. Rowat, J.H. Ipsen, Vesicle fluctuation analysis of the effects of sterols on membrane bending rigidity, Eur. Biophys. J. 33 (2004) 732–741.
[30] M.F. Hildenbrand, T.H. Bayerl, Differences in the modulation of collective membrane motions by ergosterol, lanosterol and cholesterol: A dynamic light scattering study, Biophys. J. 88 (2005) 3360–3367.
[31] K.J. Tierney, D.E. Block, M.L. Longo, Elasticity and phase behavior of DPPC membrane modulated by cholesterol, ergosterol and ethanol, Biophys. J. 89 (2005) 2481–2493.
[32] R. Krivanek, L. Okoro, R. Winter, Effect of cholesterol and ergosterol on the compressibility and volume fluctuations of phospholipid-sterol bilayers in the critical point region: a molecular acoustic and calorimetric study, Biophys. J. 94 (2008) 3538–3548.
[33] J. Pencer, M.-P. Nieh, T. Harroun, S. Krueger, C. Adams, J. Katsaras, Bilayer thickness and the thermal response of dimyristoylphosphatidylcholine unilamellar vesicles containing cholesterol, ergosterol and lanosterol: a small angle neutron scattering study, Biochim. Biophys. Acta 1720 (2005) 84–91.
[34] X. Xu, E. London, The effect of sterol structure on membrane lipid domains reveals how cholesterol can induce lipid domain formation, Biochemistry 39 (2000) 843–849.
[35] M.E. Beattie, S.L. Veatch, B.J. Stottrup, S.L. Kellar, Sterol structure determines miscibility versus melting transitions in lipid vesicles, Biophys. J. 89 (2005) 1760–1768.
[36] V. Shahedi, G. Oradd, G. Lindblom, Domain formation in DOPC/SM bilayers studied by pfg-NMR: effect of sterol structure, Biophys. J. 91 (2006) 2501–2507.
[37] R.N. McElhaney, The use of differential scanning calorimetry and differential thermal analysis in studies of model and biological membranes, Chem. Phys. Lipids 30 (1982) 229–259.
[38] T.P.W. McMullen, R.N.A.H. Lewis, R.N. McElhaney, Differential scanning calorimetric study of the effect of cholesterol on the thermotropic phase behavior of a homologous series of linear saturated phosphatidylcholines, Biochemistry 32 (1993) 516–522.
[39] T.P.W. McMullen, R.N.A.H. Lewis, R.N. McElhaney, Comparative differential scanning calorimetric and FTIR and ^{31}P-NMR spectroscopic studies of the effects of cholesterol and androstenol on the thermotropic phase behavior and organization of phosphatidylcholine bilayers, Biophys. J. 66 (1994) 741–752.
[40] T.P.W. McMullen, R.N. McElhaney, New aspects of the interactions of cholesterol and dipalmitoylphosphatidylcholine bilayers as revealed by high-sensitivity differential scanning calorimetry, Biochim. Biophys. Acta 1234 (1995) 90–98.
[41] T.P.W. McMullen, R.N.A.H. Lewis, R.N. McElhaney, Calorimetric and spectroscopic studies of the effects of cholesterol on the thermotropic phase behavior and organization of a homologous series of linear saturated phosphatidylethanolamine bilayers, Biochim. Biophys. Acta 1416 (1999) 119–234.
[42] T.P.W. McMullen, R.N.A.H. Lewis, R.N. McElhaney, Differential scanning calorimetric and Fourier transform infrared spectroscopic studies of the effects of cholesterol on the thermotropic phase behavior and organization of a homologous series of linear saturated phosphatidylserine bilayer membranes, Biophys. J. 79 (2000) 2056–2065.
[43] D.A. Mannock, T.J. McIntosh, X. Jang, D.F. Covey, R.N. McElhaney, Effects of natural and enantiomeric cholesterol on the thermotropic phase behavior and structure of egg sphingomyelin bilayers, Biophys. J. 84 (2003) 1038–1046.
[44] D.A. Mannock, R.N.A.H. Lewis, R.N. McElhaney, Comparative calorimetric and spectroscopic studies of the effects of lanosterol and cholesterol on the thermotropic phase behavior and organization of dipalmitoylphosphatidylcholine bilayer membranes, Biophys. J. 91 (2006) 3327–3340.
[45] R.N.A.H. Lewis, D.A. Mannock, R.N. McElhaney, Differential scanning calorimetry in the study of lipid phase transitions in model and biological membranes: practical considerations, in: A. Dopico (Ed.), Methods in Membrane Lipids, Humana Press, Totown, Ney Jersey, 2007, pp. 171–195.
[46] R.N.A.H. Lewis, I. Winter, M. Kriechbaum, K. Lohner, R. McElhaney, Studies of the structure and organization of cationic lipid membranes: calorimetric, spectroscopic and x-ray diffraction studies of linear saturated P-O-ethyl phosphatidylcholines, Biophys. J. 80 (2001) 1329–1342.
[47] T.P.W. McMullen, C. Vilcheze, R.N. McElhaney, R. Bittman, Differential scanning calorimetric study of the effect of sterol side chain length and structure on dipalmitoylphosphatidylcholine thermotropic phase behavior, Biophys. J. 69 (1995) 169–176.
[48] C. Vilcheze, T.P.W. McMullen, R.N. McElhaney, R. Bittman, The effect of side chain analogues of cholesterol on the thermotropic phase behavior of 1-stearoyl-2-oleoyl-phosphatidylcholine bilayers: a differential scanning calorimetric study, Biochim. Biophys. Acta 1279 (1996) 235–242.
[49] R.N.A.H. Lewis, R.N. McElhaney, FTIR spectroscopy in the study of hydrated lipids and lipid bilayer membranes, in: H.H. Mantsch, D. Chapman (Eds.), Infrared Spectroscopy of Biomolecules, John Wiley and Sons, New York, 1996, pp. 159–202.
[50] R.N.A.H. Lewis, R.N. McElhaney, The structure and organization of phospholipid bilayers as revealed by infrared spectroscopy, Chem. Phys. Lipids 96 (1998) 9–21.
[51] P.T.T. Wong, S.E. Capes, H.H. Mantsch, Hydrogen-bonding between anhydrous cholesterol and phosphatidylcholines—an infrared spectroscopic study, Biochim. Biophys. Acta 980 (1989) 37–41.
[52] D.A. Mannock, M.Y.T. Lee, R.N.A.H. Lewis, R.N. McElhaney, Comparative calorimetric and spectroscopic studies of the effects of cholesterol and epicholesterol on the thermotropic phase behaviour of dipalmitoylphosphatidylcholine bilayer membranes, Biochim. Biophys. Acta 1778 (2008) 2190–2202.